

## Delocalization and phase transitions in Pr: Theory

Per Söderlind

*Department of Physics, Lawrence Livermore National Laboratory, Livermore, California 94550*

(Received 26 July 2001; published 19 February 2002)

Density-functional electronic structure calculations have been used to investigate the high pressure behavior of Pr at low temperature. Several phase transitions are suggested by these calculations and they agree well with available experimental data. At low pressure, a dhcp (Pr-I)  $\rightarrow$  fcc (Pr-II) transition is calculated to occur at 60 kbar. Not considering the Pr-III phase, which is computationally too demanding, Pr-II transforms to the  $\alpha$ -U (Pr-IV) phase at 165 kbar. This latter transition is accompanied by a volume collapse of about 10% and is driven by delocalization of the  $4f$  electrons in Pr. The axial ratios ( $b/a$  and  $c/a$ ) and the internal parameter  $y$  of Pr-IV were calculated as a function of compression.  $y$  and  $c/a$  are rather insensitive to the compression whereas  $b/a$  decreases significantly with increasing pressure. At about 1 Mbar a new phase is predicted, namely a body-centered-tetragonal (bct) structure with a  $c/a$  axial ratio of 1.78. This new phase is stable up to very high pressures but at a sixfold compression an ultimate hexagonal close-packed (hcp) structure is predicted. The calculated high pressure behavior of Pr is similar to that of the early actinide Pa. Pressure induced increase in  $4f$ -orbital overlap, occupation and band width together with an increased electrostatic Coulomb interaction with pressure are the key components in stabilizing the high pressure phases of Pr.

DOI: 10.1103/PhysRevB.65.115105

PACS number(s): 71.20.Eh, 61.66.Bi, 64.10.+h

### I. INTRODUCTION

The rare-earth metals exhibit rich phase diagrams with several structural phase transitions when compressed.<sup>1</sup> At lower pressures the crystal-structure sequence of hexagonal close-packed (hcp), Sm-type, double hexagonal close-packed (dhcp), face-centered cubic (fcc), distorted fcc (d-fcc) is generally observed as a function of pressure. These structures are close-packed with relatively high symmetry and the transitions, understood from pressure-induced  $sp \rightarrow d$  promotion,<sup>2</sup> do not show any volume collapses. At higher pressures, new phases that are more complex with lower symmetries are often found and sometimes the transition is accompanied by a substantial volume collapse.<sup>1</sup>

Praseodymium is dhcp (Pr-I) at ambient conditions and a phase transition at room temperature to fcc (Pr-II) is observed at about 40 kbar and followed at about 70 kbar by Pr-III which is a distorted (24 atom/cell) fcc-type (d-fcc) structure.<sup>3,4</sup> Chesnut *et al.*<sup>4</sup> also argued that Pr could be described as a monoclinic cell ( $C2/m$ ) with less atoms/cell above 100 kbar. At pressures above 200 kbar, an orthorhombic phase ( $\alpha$ -U) appears and the transition to this Pr-IV phase is associated with a large volume collapse. In the literature values of this collapse have spread between 9–16.7% (Refs. 3–7) with the most recent experiment<sup>3</sup> suggesting 10.7% at 300 K. Chesnut *et al.*<sup>4</sup> studied Pr up to 1.03 Mbar, in anticipation of new phase transitions, but none was found.

Theoretically, the low pressure and high symmetry structures in Pr (and the rare earths in general) are well understood to be stabilized by the  $5d$  electrons.<sup>2</sup> The  $4f$  electrons are believed to be localized at each atom with very little involvement in the chemical bonds. At higher pressures, however, the narrow  $4f$  bands overlap more and their interatomic interaction increase. The Pr-III  $\rightarrow$  Pr-IV transition and the associated large volume collapse suggests a sudden participation of  $4f$  electrons in the chemical bond. Also a loss of

local magnetic moment on the  $f$  site follows the transition and in the Mott transition model<sup>8</sup> this is due to quenching of the  $f$ -shell moment. Hence, the Pr-III  $\rightarrow$  Pr-IV is an electronic structure transition that likely is the cause of the structural transition. Although the low-pressure phases of Pr is well understood, this volume-collapse transition has been more challenging for theory. Recent developments in density-functional theory, however, have made it possible to calculate the main features of such a transition with reasonable accuracy. Some success have been reported using so-called self-interaction correction (SIC) as well as orbital polarization (OP) techniques for the Pr-III  $\rightarrow$  Pr-IV transition in praseodymium<sup>9</sup> but Pr has not been studied theoretically at pressure above about 200 kbar.

At pressures beyond the Pr-III  $\rightarrow$  Pr-IV transition, praseodymium is believed to be an itinerant  $4f$  metal similar to Ce at high pressures or the light actinides, Th-Pu ( $5f$ ), at ambient conditions. In these systems, the  $f$  bands dominate the bonding and the structural behavior under pressure has been theoretically investigated in detail.<sup>10</sup> The narrow  $f$  band, positioned close to the Fermi level ( $E_F$ ), drives a Peierls or Jahn-Teller-like distortion of the lattice.<sup>11</sup> Symmetries of the lattice give rise to degeneracies and high density of  $f$ -electron states in the vicinity of  $E_F$ . This is energetically unfavorable and a lower symmetry structure is preferred. The number of  $f$  electrons involved in this mechanism is, of course, important. For Ce and Th, with about one  $f$  electron or less at ambient pressure, the effect is small and they are stable in a high symmetry fcc phase. For Pa-Pu, which gradually are filling the  $5f$  band, this symmetry breaking mechanism becomes increasingly important. Pa is body-centered tetragonal (bct), U orthorhombic (2 atoms/cell), Np orthorhombic (8 atoms/cell), and Pu monoclinic (16 atoms/cell). Applied pressure to these metals will have three dominating effects; (i) an  $spd$  promotion to the  $f$  band, (ii) a broadening of the  $f$  band, and (iii) an increase in electrostatic energies. (i) drive transitions to *lower* symmetry structures

such as bct in Ce and Th, (Ref. 12) and  $\alpha$ -U in Pa.<sup>13</sup> (ii) and (iii) drive transitions to *higher* symmetry structures such as hcp in Ce, Th, and Pa, bct and bcc in U and bcc in Np and Pu.<sup>10</sup> In the itinerant  $4f$  regime, Pr is the analog of the  $5f$  metal Pa (similar amount of  $f$  electrons, see below) and therefore expected to behave similarly under pressure. Pa is predicted<sup>10</sup> to undergo transitions,  $bct \rightarrow \alpha\text{-U} \rightarrow bct \rightarrow hcp$  as a function of pressure. Pr-IV ( $\alpha$ -U) is likely to undergo a transition to a new bct phase at sufficiently high pressure due to the effects (ii) and (iii) above and in analogy with Pa. At even higher pressures it seems plausible that Pr, again in analogy with Pa, will crystallize in an hcp structure.

The motivation of the paper is to study the structural behavior of Pr as a function of pressure at low temperature. At lower pressures the theory will be tested by comparisons with experimental data. At pressures beyond the Pr-III  $\rightarrow$  Pr-IV transition (about 200 kbar) we expect a behavior similar to that of Pa, i.e., phase transitions to gradually higher symmetry structures.

The article is organized as follows. Section II deals with computational details and is followed by a presentation of our results in Sec. III. In Sec. IV we discuss our results and comment upon future studies.

## II. COMPUTATIONAL DETAILS

The total energy for Pr-I (dhcp), Pr-II (fcc), Pr-IV ( $\alpha$ -U), hcp, bcc, and bct for Pr was calculated as a function of volume. The experimentally suggested Pr-III phase is a distorted cell with many atoms per cell (24) which make theoretical consideration of this phase very difficult and we chose not to calculate the energies for this phase. Therefore, also the suggested competing monoclinic ( $C2/m$ ) phase,<sup>4</sup> is only briefly studied.

The dhcp structure was calculated using an ideal packing  $c/2a$  ratio (1.633). The  $\alpha$ -U structure is orthorhombic with axial ratios  $b/a$ ,  $c/a$  and an internal parameter  $y$  which were all optimized at each volume. Also the bct  $c/a$  ratio was optimized at each volume. bcc, fcc, bct, and  $\alpha$ -U structures were all calculated for a common 2 atom/cell orthorhombic geometry to maximize cancellation of errors in differences of their total energies. Test calculations for the  $C2/m$  structure were performed with structural parameters fixed to those given by Chesnut *et al.*<sup>4</sup>

For these calculations we used the full potential version of the linear muffin-tin orbital method (FP-LMTO).<sup>14</sup> This electronic structure method is an implementation of density-functional theory as applied for a bulk material. It is a first-principle method, no experimental numbers are used in the calculations except for the nuclear charge which is 59 for Pr. The approximations in this approach are limited to the approximation of the exchange/correlation energy functional, cut offs in the expansion of basis functions,  $k$ -point sampling in integrations over the Brillouin zone, and the Born-Oppenheimer approximation. For the exchange/correlation approximation we used the generalized gradient approximation (GGA) which has proven to be better for  $f$ -electron metals than the more commonly used local density approximations.<sup>15</sup> Spin-orbit coupling and spin/orbital polar-

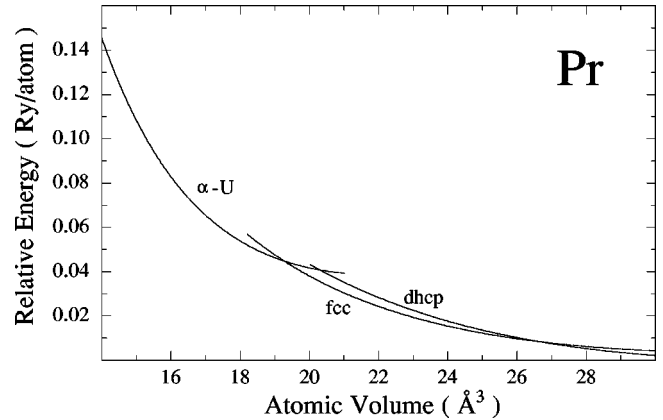


FIG. 1. Murnaghan (Ref. 17) equation-of-state as fitted to calculated total energies of Pr in the dhcp, fcc, and  $\alpha$ -U crystal structures. Calculated transition pressures; dhcp  $\rightarrow$  fcc: 60 kbar, and fcc  $\rightarrow$   $\alpha$ -U: 165 kbar. There is a negligible volume collapse at the first transition but a 10.2% volume collapse at the second transition.

ization were allowed for, in the same way as have been described earlier,<sup>9</sup> and only ferromagnetic order was considered.

The use of full nonsphericity of the charge density and one-electron potential is essential for accurate total energies. This is accomplished in our method by expanding charge density and potential in cubic harmonics inside nonoverlapping muffin-tin spheres and in a Fourier series in the interstitial region. In all calculations we used two energy tails associated with each basis orbital and for  $5s$ ,  $5p$ , and the valence states ( $6s$ ,  $6p$ ,  $5d$ , and  $4f$ ) these pairs were different. With this “double basis” approach we used a total of six energy tail parameters and a total of 12 basis functions per atom. Spherical harmonic expansions were carried out through  $l_{\max}=8$  for the bases, potential, and charge density. The sampling of the irreducible Brillouin-zone was done using the special  $k$ -point method<sup>16</sup> and the number of  $k$  points we used was 250 for bcc, fcc, bct, and  $\alpha$ -U. For dhcp and hcp we used 102, and 476  $k$  points, respectively, and for the  $C2/m$  structure 216  $k$  points. To each energy eigenvalue a Gaussian was associated with 20 mRy width to speed up convergence. Total energy calculations were carried out for each crystal structure as a function of volume. These energies were then fitted to a Murnaghan equation of state (EOS) which enabled us to calculate the Gibbs free energy,

$$G = E + PV - TS = H - TS \quad (1)$$

for the considered structures of Pr. Here  $H$ ,  $S$ , and  $E$  are the enthalpy, entropy, and internal energy of the system. In our calculations  $T=0$  and  $E$  is the total (electronic) energy. A phase transition between two phases occurs if their Gibbs free energy coincides for a given pressure. Using the EOS (pressure as a function of volume) for the two phases we are able to calculate the volume collapse associated with the transition.

## III. RESULTS

In Fig. 1 we show the total energies for dhcp, fcc, and the

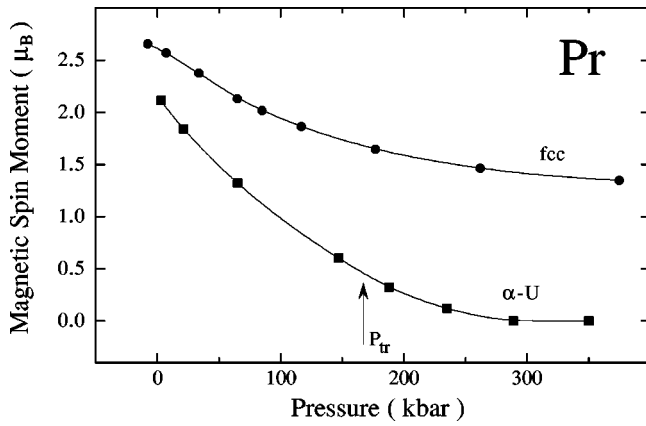


FIG. 2. Calculated spin moment for Pr in the fcc and  $\alpha$ -U structure as a function of pressure. The volume-collapse transition (see main text) is denoted by  $P_{tr}$ .

$\alpha$ -U phase of Pr for moderate compression. A Murnaghan<sup>17</sup> fit to the ground-state dhcp energies gives an equilibrium volume  $V_0=33.4 \text{ \AA}^3$  and a bulk modulus  $B=258$  kbar. The calculated total (spin and orbital) magnetic moment is  $0.9\mu_B$  at equilibrium. The EOS data compares well with the most recent experimental data<sup>3</sup> ( $V_0=34.5 \text{ \AA}^3$  and  $B=259$  kbar) but the size of the magnetic moment is somewhat large compared to data obtained from neutron scattering ( $0.36\mu_B$ ).<sup>18</sup>

Notice in Fig. 1 two transitions, the first transition (Pr-I/Pr-II) dhcp  $\rightarrow$  fcc is calculated to occur at about 60 kbar with a negligible volume collapse. At 165 kbar calculations reveal another phase transition, fcc  $\rightarrow$   $\alpha$ -U with an associated volume collapse of 10.2%. The experimental room temperature pressures<sup>3</sup> for the (Pr-I/Pr-II) transition is about 40 kbar, (Pr-II/Pr-III) about 70 kbar, and for the (Pr-III/Pr-IV) transition about 200 kbar. The volume collapse for the (Pr-III/Pr-IV) transition measured in the most recent experiment<sup>3</sup> is 10.7% which is in good agreement with the calculated fcc  $\rightarrow$   $\alpha$ -U volume collapse. Baer *et al.*<sup>3</sup> present the Pr-I/Pr-II and the Pr-III/Pr-IV phase lines in their paper which enable us to extrapolate the transition pressures to zero temperature. These extrapolated pressures are 55 and 165 kbar which compares well with the corresponding theoretical pressures of 60 and 165 kbar.

At all volumes, the axial ratios and the internal parameter of the  $\alpha$ -U structure were optimized and at volumes close to the volume-collapse transition  $c/a=1.812$ ,  $b/a=2.025$ , and  $y=0.10$ . These data agree well with known experimental data at 269 kbar and 718 K ( $c/a=1.784$  and  $b/a=2.000$ ).<sup>3</sup> Baer *et al.* did not report any value of  $y$  but Chesnut *et al.*<sup>4</sup> found that  $y=0.1$  gave the best fit to their diffraction intensities in a wide pressure range.

In addition to the structural properties it is of interest to also study the magnetic behavior of Pr, see Fig. 2. At low pressures both Pr-II and Pr-IV have a spin moment over  $2\mu_B$ . This can be compared with the measured (4.2 K) saturated moment of  $2.7$ .<sup>19</sup> The spin moment is gradually suppressed with increasing pressure and for the  $\alpha$ -U phase the spin moment collapses rather rapidly. Close to the volume-collapse transition ( $P_{tr}$ ) fcc Pr has still a substantial spin

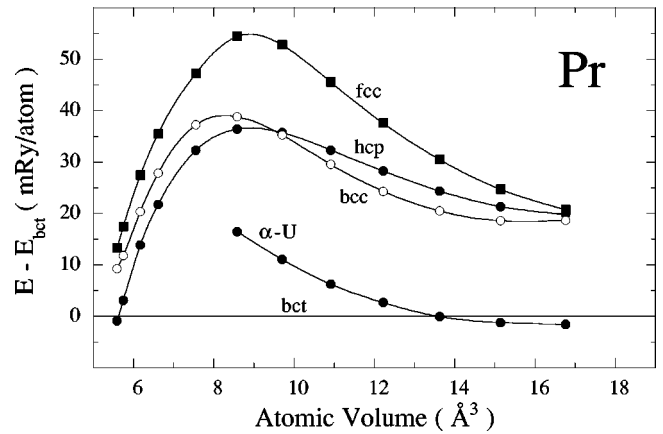


FIG. 3. Total energies of Pr in the bcc, hcp, fcc, and  $\alpha$ -U structures relative to bct Pr. Energy differences are denoted by symbols, connecting lines are guides for the eye only.

moment of  $1.7\mu_B$ , whereas the spin moment is almost quenched for the  $\alpha$ -U phase ( $0.45\mu_B$ ). A calculation where the spin moment is constrained to zero reveals that the effect on the total energy of this small spin moment for the  $\alpha$ -U phase is in fact very small (0.4 mRy/atom) and close to our computational accuracy. Calculations of the  $C2/m$  structure,<sup>4</sup> at volumes close to the fcc  $\rightarrow$   $\alpha$ -U transition, reveal that the spin moment of this structure is identical to the fcc structure and their respective total energies are close with the fcc energy being about 1 mRy/atom lower. The  $\alpha$ -U phase, on the other hand, has a nearly quenched magnetic moment at these volumes. If we interpret the loss of magnetic moment as a signature of  $f$  delocalization, the  $C2/m$  structure does not seem to be a phase that is stabilized by itinerant  $4f$  electrons.

In Fig. 3 we focus on higher compressions of Pr. Here we present the total energies relative to the bct structure to more clearly show the energy differences between the various phases. Notice that the total energy of the bct phase is very close to that of the  $\alpha$ -U phase and that these energies are almost parallel functions of volume up to the  $\alpha$ -U  $\rightarrow$  bct ( $c/a=1.78$ ) transition that occurs at about  $13.7 \text{ \AA}^3$ . This makes the calculated transition pressure, 1.04 Mbar, somewhat sensitive to the computational accuracy. The axial ratios of the bct and  $\alpha$ -U structures were optimized as well as the atomic coordinate  $y$  ( $\alpha$ -U). All internal parameters vary continuously and monotonically with increasing compression. In Fig. 4 we show the volume dependence of the  $c/a$  axial ratio for bct Pr. The  $c/a$  ratio is about 1.85 at  $17 \text{ \AA}^3$  and decreases continuously to about 1.6 at  $6 \text{ \AA}^3$ . For the  $\alpha$ -U phase,  $b/a$  is more sensitive to volume compression than are  $c/a$  and  $y$ . At  $20 \text{ \AA}^3$   $b/a$  is 2.025 and at  $8 \text{ \AA}^3$  this axial ratio has decreased to 1.90. The  $c/a$  ratio is close to constant in this interval increasing somewhat from 1.812 to 1.85 and  $y$  also increases marginally from 0.10 to about 0.11. Chesnut *et al.* measured  $c/a=1.81$ ,  $b/a=1.99$  at 1.03 Mbar which compares well with our calculated  $c/a=1.85$ ,  $b/a=1.95$  at 1.04 Mbar. Chesnut *et al.*<sup>4</sup> also obtained an atomic volume of  $14.0 \text{ \AA}^3$  at 1.03 Mbar in good agreement with our calculated atomic volume of  $13.7 \text{ \AA}^3$  at 1.04 Mbar.

Notice further in Fig. 3 that at initial compression the high

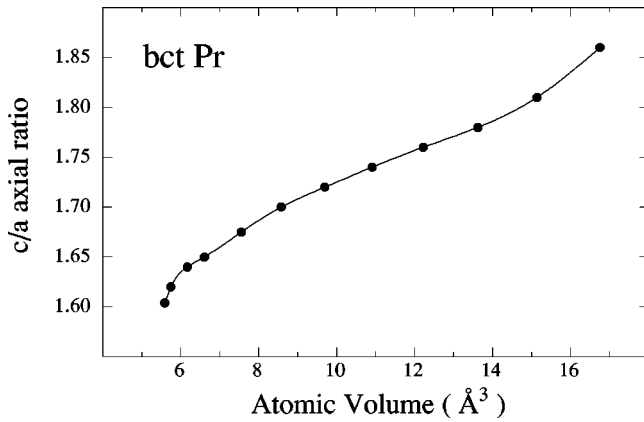


FIG. 4. Calculated  $c/a$  axial ratio for bct Pr as a function of atomic volume.

symmetry structures bcc, fcc, and hcp are all increasingly unfavorable compared to both the lower symmetry phases, bct and  $\alpha$ -U. By calculating the total energies along the so-called Bains path (a tetragonal distortion of the bct structure), see Fig. 5, we can deduce that both bcc and fcc are in fact mechanically unstable at about  $17 \text{ \AA}^3$ . At extreme compression, however, the high symmetry structures become more competitive and eventually hcp is predicted to be the stable phase in Pr. The axial  $c/a$  ratio for hcp was kept equal to its ideal-packing value (1.633) for most volumes, but for the most compressed volumes this ratio was optimized. At about  $6 \text{ \AA}^3$   $c/a$  was calculated to be 1.61.

#### IV. DISCUSSION

The electronic structure of praseodymium is naturally divided into two regimes. The first, low-pressure (localized), regime is categorized by lack of  $4f$  participation in the chemical binding and the  $5d$  electrons instead dominate the bonding. This results in, for instance, close-packed and high symmetry structures with a low density and bulk modulus. Phases in this regime are Pr-I, Pr-II, and Pr-III. In the second

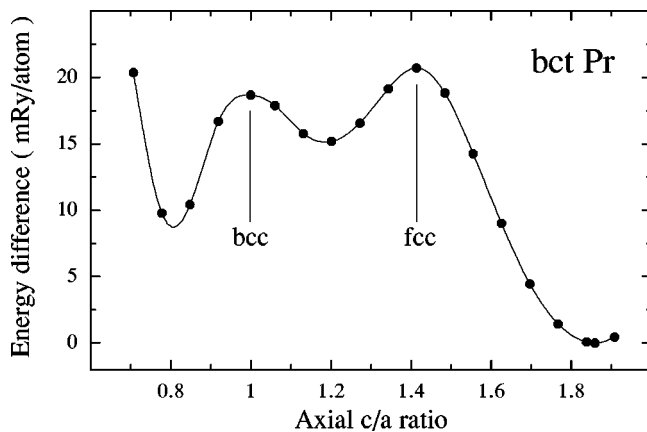


FIG. 5. Energy differences, relative to the total energy minimum, for bct Pr as a function of  $c/a$  axial ratio at about  $17 \text{ \AA}^3$ . bcc and fcc corresponds to  $c/a=1$  and  $\sqrt{2}$ , respectively. Connecting line is guide for the eye only.

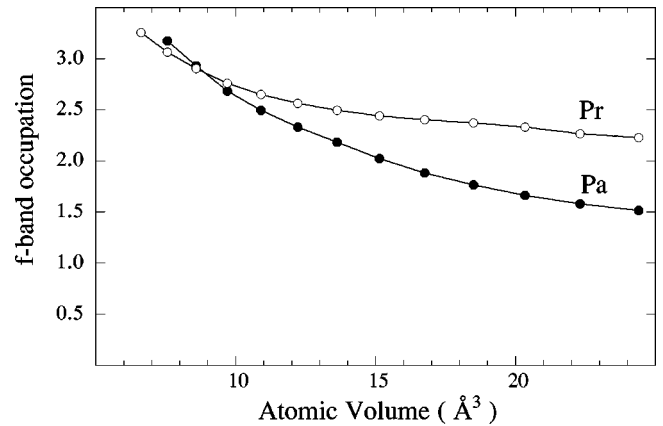


FIG. 6. Calculated  $f$ -band occupation numbers (inside muffin-tin spheres, see main text) fcc Pr and fcc Pa.

(itinerant) regime the  $4f$  electrons behave as band electrons and as a result, the lattice collapses to a low symmetry structure with higher density and bulk modulus. The first phase in this regime is Pr-IV ( $\alpha$ -U).

We have shown above that both the localized and the itinerant regimes of Pr can be well described from first-principles theory. For the localized regime, theory predict the correct ground-state (dhcp) and equilibrium volume and bulk modulus are both in good agreement with experiment with  $-3$  and  $0\%$  relative errors, respectively. The Pr-I $\rightarrow$ Pr-II phase transition is, when extrapolated to zero temperature,  $55 \text{ kbar}$  which compares well with our calculated value of  $60 \text{ kbar}$ . Theory and experiment also agree that there is no significant volume change at this transition.

For the itinerant regime, theory correctly predict the first stable phase, Pr-IV ( $\alpha$ -U). The magnetic calculations indicate a small, but for all practical purposes negligible, spin moment for Pr-IV at the transition. This confirms that the  $4f$  electrons are indeed itinerant and nonmagnetic theory applies well at this pressure and beyond. The measured Pr-III/Pr-IV transition pressure, when extrapolated to zero temperature, is in exact agreement with theory ( $165 \text{ kbar}$ ) for the fcc  $\rightarrow \alpha$ -U transition. The error introduced by not considering the correct (d-fcc) Pr-III phase for this transition is believed to be small because the equation-of-state for Pr-II and Pr-III are known to be very similar.<sup>3</sup> Calculated axial ratios and internal coordinate of Pr-IV are sensitive properties that also agree well with experiment. Theoretical atomic volume of this phase at about  $1 \text{ Mbar}$  is again in very good agreement with experiment.

Thus, our theory is capable of reproducing the known behavior of Pr under compression. In addition, theory predicts two new high pressure phases of Pr, namely, bct and hcp. The bct phase transition is calculated to occur at  $1.04 \text{ Mbar}$  which is just beyond the highest studied pressure for Pr. The hcp phase occurs at some very large pressure, well beyond experimental capability, at about a sixfold compression.

At high pressures, beyond the Pr-III/Pr-IV transition, Pr is calculated to adopt the crystal structure sequence  $\alpha$ -U $\rightarrow$ bct $\rightarrow$ hcp. This sequence has also been predicted for the light actinide Pa.<sup>13</sup> The reason to this behavior has been discussed

before<sup>10</sup> and is due to the fact that the  $f$  bands broaden and electrostatic interactions increase at high volume compression. This will gradually stabilize higher symmetry structures with increasing pressure and therefore explain the  $\alpha$ -U  $\rightarrow$  bct transition. However, a higher symmetry structure such as bcc, fcc, or hcp is expected as the ultimate high pressure phase. The electrostatic energy differences between these structures are small and band filling effects will distinguish them at high pressures. In an earlier study of the light actinides and Ce<sup>10</sup> it was shown that canonical band theory could be used to estimate the preferred structure once the  $f$ -band occupation is known. For Ce, Th, and Pa, this model predicted the hcp phase as the ultimate high pressure phase.<sup>10</sup> Pr, at pressures beyond the volume-collapse transition, is an itinerant  $4f$  system with  $f$ -band occupancy very similar to that of Pa, see Fig. 6. This figure shows the calculated  $f$ -band occupation as a function of volume for fcc Pr and fcc Pa. The occupation number is calculated within the muffin-tin spheres which here constitutes about 70% of the lattice volume. Notice that at smaller volumes the difference in  $f$ -band

occupation between Pr and Pa is less than half an  $f$  electron. At high compressions one could therefore suspect that Pr and Pa would behave in a similar fashion. Calculations indeed support this notion, theoretical phase transition in Pa are bct  $\rightarrow$   $\alpha$ -U  $\rightarrow$  bct  $\rightarrow$  hcp, i.e., the latter two transitions are the same as those we have calculated for Pr-IV.

The collapsed phases of Ce and Pr are clearly analogous to the light actinides Th and Pa. Similarly, Nd is believed to be a  $4f$  analog of uranium at sufficiently high pressure. U is predicted to undergo phase transitions to the bct and bcc structures at high compression.<sup>10</sup> This scenario is likely to occur also for Nd and theoretical calculations are underway to explore this speculation.

#### ACKNOWLEDGMENTS

Valuable discussions with H. Cynn is acknowledged. This work was performed under the auspices of the U.S. Dept. of Energy at the University of California/Lawrence Livermore National Laboratory under Contract No. W-7405-Eng-48.

- 
- <sup>1</sup>A.K. McMahan, C. Huscroft, R.T. Scalettar, and E.L. Pollock, *J. Comput.-Aided Mater. Des.* **5**, 131 (1998).  
<sup>2</sup>J.C. Duthie and D.G. Pettifor, *Phys. Rev. Lett.* **38**, 564 (1977); A.K. McMahan, H.L. Skriver, and B. Johansson, *Phys. Rev. B* **23**, 5016 (1981).  
<sup>3</sup>B.J. Baer, H. Cynn, V. Iota, C.-S. Yoo, and G. Shen (unpublished).  
<sup>4</sup>G.N. Chesnut and Y.K. Vohra, *Phys. Rev. B* **62**, 2965 (2000).  
<sup>5</sup>G.S. Smith and J. Akella, *J. Appl. Phys.* **53**, 9212 (1982).  
<sup>6</sup>Y.C. Zhao, F. Porsch, and W.B. Holzapfel, *Phys. Rev. B* **52**, 134 (1995).  
<sup>7</sup>W.A. Grosshans, Y.K. Vohra, and W.B. Holzapfel, *J. Phys. F* **13**, L147 (1984).  
<sup>8</sup>B. Johansson, *Philos. Mag.* **30**, 469 (1974).  
<sup>9</sup>A. Svane, J. Trygg, B. Johansson, and O. Eriksson, *Phys. Rev. B* **56**, 7143 (1997).  
<sup>10</sup>P. Söderlind, *Adv. Phys.* **47**, 959 (1998).  
<sup>11</sup>P. Söderlind, O. Eriksson, B. Johansson, J.M. Wills, and A.M. Boring, *Nature (London)* **374**, 524 (1995).  
<sup>12</sup>P. Söderlind, O. Eriksson, B. Johansson, and J.M. Wills, *Phys. Rev. B* **52**, 13 169 (1995).  
<sup>13</sup>P. Söderlind and O. Eriksson, *Phys. Rev. B* **56**, 10 719 (1997).  
<sup>14</sup>J.M. Wills (unpublished); J.M. Wills and B.R. Cooper, *Phys. Rev. B* **36**, 3809 (1987); D.L. Price and B.R. Cooper, *ibid.* **39**, 4945 (1989).  
<sup>15</sup>J.P. Perdew, J.A. Chevary, S.H. Vosko, K.A. Jackson, H.R. Pederson, D.J. Singh, and C. Fiolhais, *Phys. Rev. B* **46**, 6671 (1992).  
<sup>16</sup>D.J. Chadi and M.L. Cohen, *Phys. Rev. B* **8**, 5747 (1973); S. Froyen, *Phys. Rev. B* **39**, 3168 (1989).  
<sup>17</sup>F.D. Murnaghan, *Proc. Natl. Acad. Sci. U.S.A.* **30**, 244 (1944).  
<sup>18</sup>H.B. Moller, J.Z. Jensen, M. Wulff, A.R. Mackintosh, O.D. McMasters, and K.A. Gschneidner, Jr., *Phys. Rev. Lett.* **49**, 482 (1982).  
<sup>19</sup>K.A. McEwen, *Handbook on the Physics and Chemistry of Rare Earths* (North-Holland, Amsterdam, 1978), Vol. 1.